Miniature Antennas and Arrays Embedded within Magnetic Photonic Crystals and Other Novel Materials

John L. Volakis, Kubilay Sertel, and Chi-Chih Chen

ElectroScience Laboratory, Electrical and Computer Engineering Dept.
The Ohio State University
1320 Kinnear Rd., Columbus, OH 43212 USA; Email: volakis@ece.osu.edu

Abstract — Engineered materials, such as new composites, electromagnetic bandgap and periodic structures have been of strong interest in recent years due to their extraordinary and unique electromagnetic behaviors. This paper will address how modified materials, inductive/capacitive lumped loads and low loss magnetic materials/crystals are impacting antenna design with the goal of overcoming miniaturization challenges (viz. bandwidth and gain reduction, multi-functionality etc.). Dielectric design and texturing for impedance matching has, for example, led to significant size reduction and higher bandwidth low frequency antennas. Examples showing a factor of 2 or more reduction in ultrawideband antennas will be shown and operating down to nearly 100MHz using a 6" aperture. A recently introduced new class of magnetic photonic crystals (MPCs) and Degenerate Band Edge (DBE), displaying spectral nonreciprocity are also introduced. Studies of these crystals have demonstrated that MPCs exhibit the interesting phenomena of (a) drastic incoming wave slow down, coupled with (b) significant amplitude growth while (c) maintaining minimal reflection at the interface with free space. The phenomena are associated with diverging frozen modes that occur around the stationary inflection points within the band diagram. Taking advantage of the frozen mode phenomena, we demonstrate that individual antenna elements and linear or volumetric arrays embedded within the MPC and DBE structures allow for supergain effects that can lead to novel miniature (high sensitivity and high gain antennas and sensors) array configurations.

I. INTRODUCTION

Engineered materials, such as new composites, electromagnetic bandgap [1], [2], and periodic structures have attracted considerable interest in recent years due to their remarkable and unique electromagnetic behavior. As a result, an extensive literature on the theory and application of artificially modified materials has risen. Already photonic crystals have been utilized in RF applications such as waveguides, filters, and cavities due to their extraordinary propagation characteristics [3]-[8]. One of the most interesting properties associated with photonic crystals relates to their high Q resonances, achieved when a defect is introduced within the periodic structure. When an antenna element is placed within the high Q cavity, it is then possible to harness the high fields and generate exceptional gain. Experiments have already demonstrated this enhanced gain by placing small radiating elements into a cavity built around a photonic crystal. Specifically, Temelkuran, et.al. [7] and Biswas, et.al. [8] reported a received power enhancement by a factor of 180 at the resonant frequency of the cavity.

More recently, computations using double-negative materials [9] illustrate that extraordinary gain can also be achieved when small dipoles are placed inside other exotic materials that exhibit resonance at specific frequencies [10]. However, an issue with the double negative and left-handed materials is their practical realization. In this paper, we present a new class photonic crystals [9]-[18] fabricated from available material structures such as rutile, alumina, titanates and CVGs. Of importance is that these crystals exhibit much larger gain without requiring excessive volume. As such, they may be applicable for hand held devices. Of importance is also their greater bandwidth and improved matching (due to their resonance away from the band edge). Specifically (see Fig. 1), they combine the two unique properties of (i) minimal reflection at the interface of the periodic assembly forming the crystal, implying impedance matching, and (ii) wave slow down leading to miniaturization, and concurrently causing large amplitude growths within the material. The latter is of importance in realizing high gain antennas using smaller volumes. Recent computational examples have demonstrated a gain increase of as much as 15 dB for a small dipole placed within the crystal [14]. Experiments using periodic assemblies of FSS that realize the desirable band-diagram have also validated this gain increase.

The paper discusses some of these successes and proceeds with a discussion on the challenges of fabricating high contrast materials, their loss properties, and their integration with printed antennas.

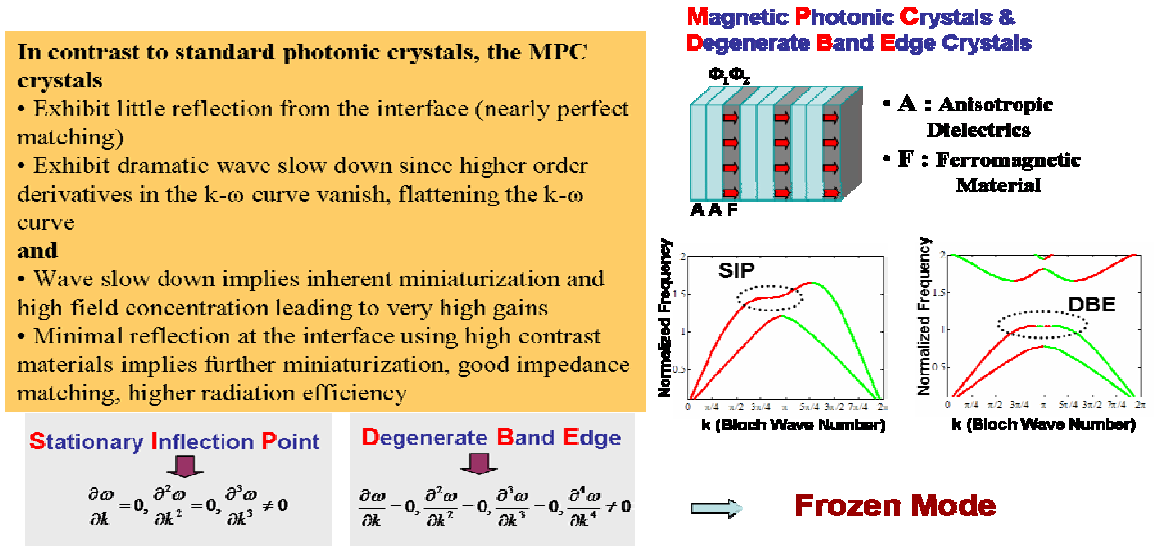

Fig. 1. Properties of the magnetic photonic crystals (MPC) and their related Degenerate Band Edge (DBE) crystals formed by a periodic array of 3-layer unit cells. MPCs require at least one layer of magnetic materials whereas the DBEs are non-magnetic and therefore easily realizable. Both, MPCs and DBEs require the presence of anisotropy to realize their unique band diagrams.

The potential of fabricating printed microstrip lines that exhibit the same band diagram is a recent discovery that could lead to a variety of miniature microwave components as well as high sensitivity sensors. We begin below by noting that even properly designed materials with embedded inductive loadings can have significant impact in reducing antenna size and improving bandwidth properties. These modifications can be easily done and can be integrated into existing systems without much increase in cost for their adaptation.

II. MINIATURE ULTRAWIDEBAND ANTENNAS USNG INDUCTIVE AND MATERIAL LOADING

Novel inductive loading within polymer structures has shown to be extremely effective in reducing antenna size, with particular emphasis on conformal installations. The motivation for using inductive loading comes from the need to emulate magnetic materials [21], [22]. By introducing inductive loading (capacitive loading is typically inherent to the structure), the antenna impedance can be matched as the antenna is miniaturized by increasing the dielectric loading. Our initial approach to implementing inductive loading was based on the artificial transmission line (ATL) miniaturization technique [21], [23]. The ATL concept of implementing inductive loading utilized distributed serial inductor elements to increase the inductance of the antenna. Avoiding use of chip inductors is critical since we need to suppress inherent losses. An alternative way to implement inductive loading is by coiling the spiral arm such that it resembles a helix as shown in Fig. 2 for a 6 inch diameter spiral antenna. Here, the coiled section of the spiral arm has a rectangular cross section which allows us to control the inductance of the coil using the pitch, width and thickness of the coil separately. In this case, the thickness remains constant while the width and pitch are varied to create a smooth transition from the untreated portion to the inductive section of the spiral arm.

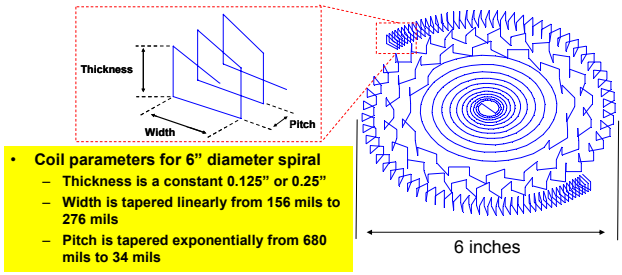

Fig. 2. Implementing inductive loading within a spiral antenna by coiling the conductor as it concurrently spirals away from the center.

We proceeded to use the concept of volumetric inductive loading via coiling [23], [24] to implement the wave slow down and miniaturization. The performance improvement is shown in Fig. 3, and shows that we have indeed achieved a 6" design that operates down to 130 MHz (-15 dBic gain) that is only λ/15 in size, and 7.5 times smaller than the nominal λ/2 dipole. Of importance is that the frequency has shifted from 320 MHz down to 130 MHz with the same performance (nearly a factor of 2.5 reduction in frequency performance). Remarkably, we are also seen to approach the theoretical limit of miniaturization for a given aperture size [23], [25], [26].

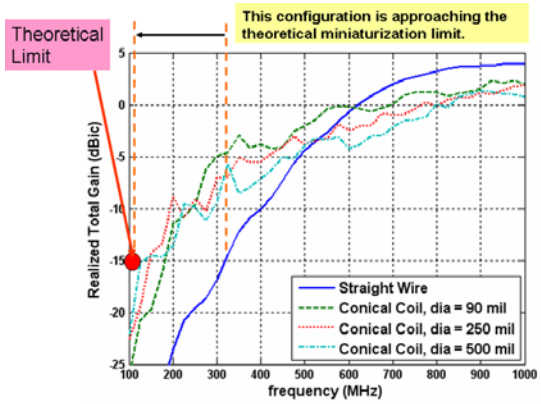

Fig. 3. Using coiling to shift antenna performance to lower frequencies.

The inductively loaded 6" spiral shown in Fig. 2 was also manufactured and measured along with a composite metal-magnetic ground plane. The assembled antenna is shown in Fig. 4(a) and has a total thickness of 1.5". The 6" spiral was fabricated on a 0.25 inch thick Roger's TMM4 substrate ($\varepsilon_r = 4.5$) using standard printed circuit board manufacturing technology. The measured realized gain is shown in Fig. 4(c) along with the measured gain of a non-miniaturized spiral antenna backed by a metallic ground plane. This plot clearly demonstrates the superior performance of the miniaturized spiral below 600 MHz. For these frequencies, the miniaturized spiral with ferrite backing is able to achieve 5-10 dBi more gain than the non-miniaturized spiral. Because the spiral is a frequency independent antenna, the antenna can be scaled to any aperture size to meet the desired specifications. For instance, Fig. 4 (b) also shows the analytical performance (free space) of the 6" aperture in addition to two scaled versions that are 9" and 12" in diameter. From Fig. 4(b), the 12" aperture is seen to operate down to 80 MHz at the -15 dBic gain and to 110 MHz at the -10 dBic gain point. Again, we also show the theoretical limit point for the 12" aperture, and note that it is close to the achieved performance.

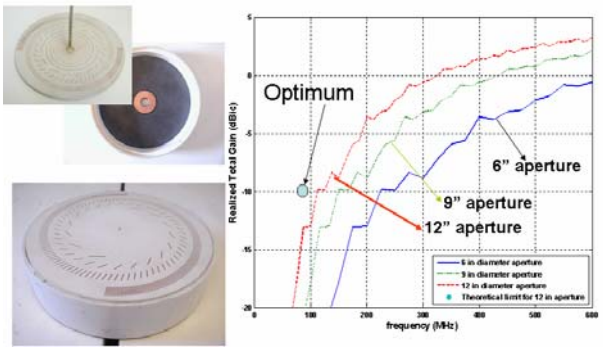

(a) **(b)**

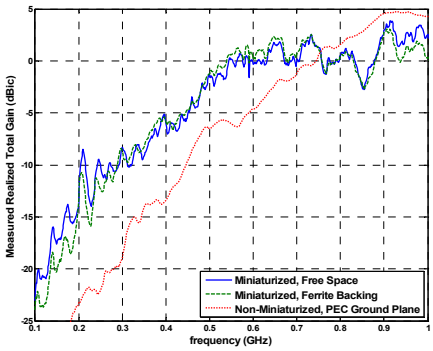

(c)

Fig. 4. Display of fabricated antenna articles incorporating volumetric coiling within dielectric loading and over a magnetic-PEC ground plane; Top left: 6" fabricated antenna 1.5" thick; Bottom: measurement results with and without ferrite backing.

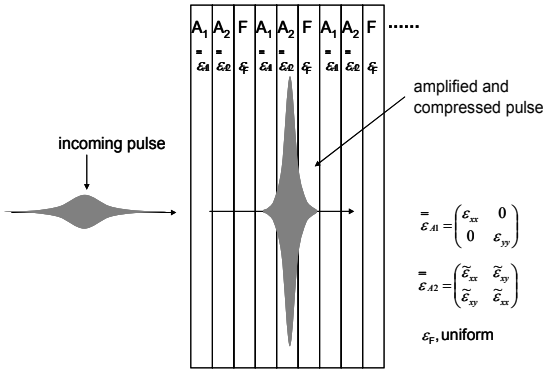

Fig. 5. Field compression within the MPC crystal: An incident pulse propagating towards right couples into the MPC and excites the frozen mode within the crystal.

III. VOLUMETRIC CRYSTALS FOR HIGH GAIN NARROW BAND ANTENNAS

MPC and DBE crystals have been pursued because they allow for further miniaturization and higher gains. However, so far, their promise has only been demonstrated for narrowband antennas. In [14], we demonstrated that the so-called *frozen mode* can indeed be realized in finite thickness magnetic photonic assemblies (MPCs) using a practical combination of materials. This mode is shown in Fig. 5. As displayed, the incoming pulse enters the periodic assembly (crystal) with very little reflection (15% of the field is typically reflected). Once in the crystal, it shows down, while it concurrently increases in amplitude by more than a factor of 10 for material with nominal losses.

A realization of the MPC and DBE crystal is shown in Fig. 6 using two misaligned anisotropic dielectric layers and an isotropic layer built into a unit cell. It was shown in [18] that it is possible to achieve a four-fold amplitude increase in the coupled electric field amplitude using 20 such unit cells to form a degenerate band edge (DBE) crystal which does not even require magnetic materials. As a direct consequence of this spatial focusing, the directivity and gain of a simple dipole antenna placed within the MPC crystal (see Fig. 7) was shown [14] to increase by 12.7 dB (~20 fold). Also shown in Fig. 7 is the effect of material loss on the overall gain of the dipole embedded within. A very slight loss of *tan* $\delta = 10^{-5}$ reduces antenna gain by only 2 dB, and this gives much promise for the practical realization of those materials.

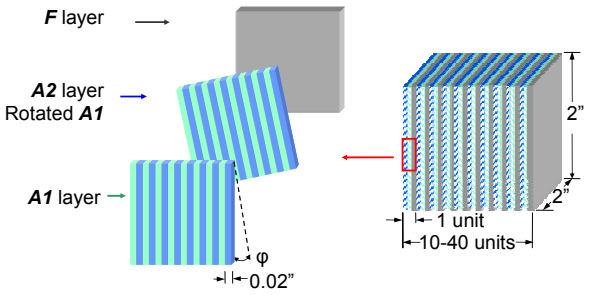

Fig. 6. MPA design: A1, A2 are two of the same anisotropic dielectric layers with φ being the misalignment angle between A1 and A2. F is the Faraday rotation ferromagnetic layer.

Of even greater importance is the realization of significant gain using periodic assemblies forming the so called DBE crystal. The fabrication of the DBE crystal can be done without magnetic materials and even more importantly using an arrangement or stacks of Frequency Selective Surfaces (FSS) surfaces as displayed in Fig. 8. In doing so, we mimicked the anisotropy in the dielectric layers by printing very thin conducting strips on low-loss Rodgers RO4350 substrate and designed the DBE band structure with proper F-layer thicknesses and misalignment angles as shown in Fig. 8. The Bloch band structure is shown in Fig. 9(a). Using a Tx-Rx antenna pair and a network analyzer, our first experiment demonstrated the existence of the regular and degenerate band edges as plotted in Fig. 9(c).

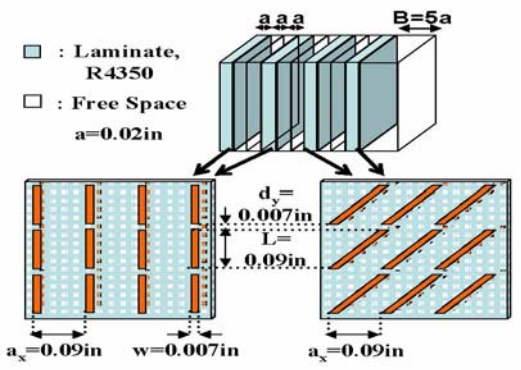

Fig. 8. DBE design using PCB technology.

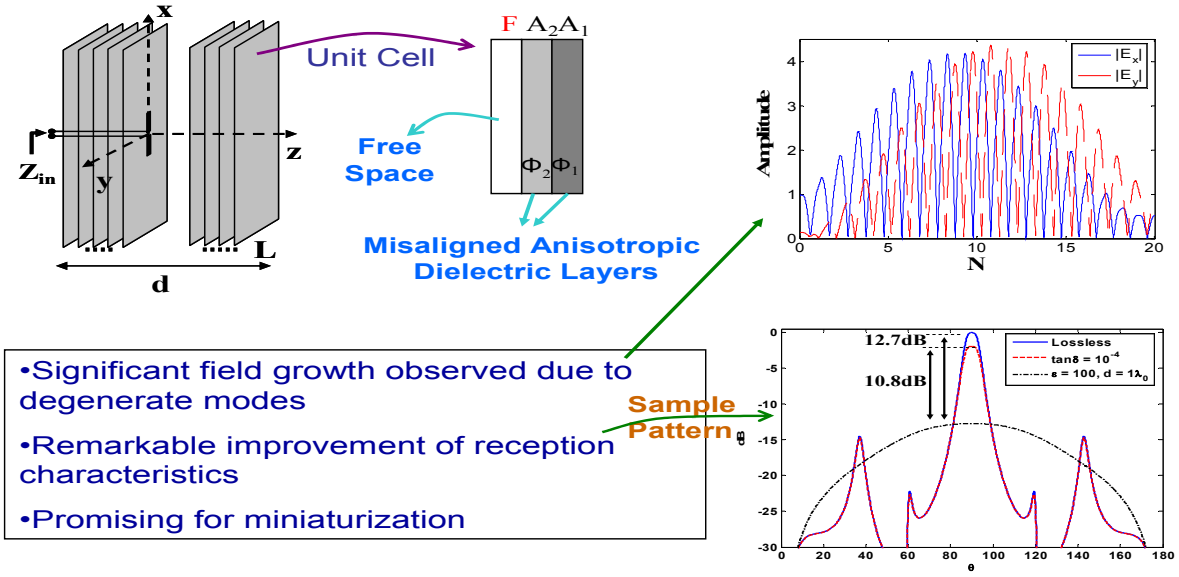

Fig. 7. Demonstration of the field amplitude growth and antenna gain realization using the non-magnetic DBE crystals (periodic assemblies).

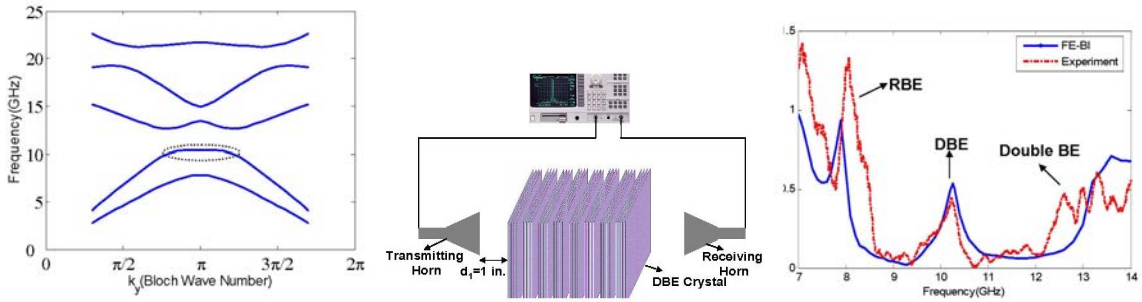

(a) **(b)** **(c)**

Fig. 9. Experimental verification of the field behavior within a DBE; (a) Designed band structure showing the DBE behavior, (b) Setup for polarimetric thru-transmission measurements using the Agilent E8362B, 10 MHz - 20 GHz PNA Series Network Analyzer, (c) Transmission through the crystal (different band edges are indicated).

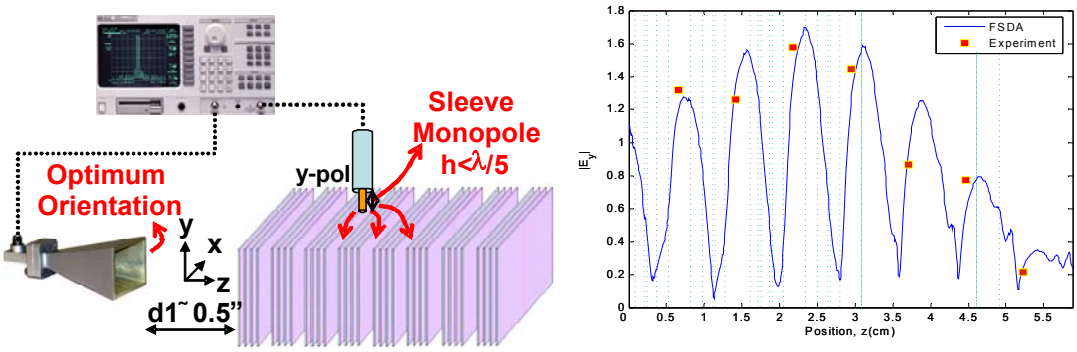

(a) **(b)**

Fig. 10. Experimental verification of the DBE Field amplitude focusing: (a) Setup for field probing measurement using the Agilent E8362B, 10 MHz – 20 GHz PNA Series Network Analyzer, (b) Calculated vs. Measured electric field strength within the DBE crystal.

Further, we proceeded to demonstrate the focusing effect of the DBE crystal via probing of the field amplitudes within each free-space layer as shown in Fig. 10. These tests provided further verification of the field amplitude growth realization and possible miniaturization afforded by the proposed MPC and DBE materials. We are currently exploring the possibility of designing the anisotropic material layers via a careful combination of isotropic building blocks as outlined below.

IV. FABRICATING PERIODIC ASSEMBLIES OF DBES AND MPCS

Practical MPCs consist of 10-40 unit cells, with each cell composed of two "A" layers rotated with respect to each other and one "F" layer, as shown in Fig. 6. To realize the predicted gains, each layer needs to be made as a thin sheet, typically of dimensions 2"×2"× 0.02", and a low dielectric loss tanδ, preferably $<10^{-5}$. Examples of possible sheet materials are rutile single crystals for the A layers, and Ca, V-doped Yttrium Iron Garnet ceramics (CVGs) for the F layer. However the rutile crystals are not available with the desired 2" × 2" dimensions and their cost may prohibit practical realization. In addition, the measured losses of commercially available rutile crystals are $>10^{-4}$ while there is little opportunity to improve this number by modifying the composition. The properties of commercially available CVG materials are promising but are yet to be explored for this application and further developed. Little is also know about the compatibility and manufacturability of these materials into an operational device. These factors have inhibited the realization of a prototype. To overcome these issues we have been working with Prof. Verweij (Material Science Dept. at The Ohio State University)[1] on approaches as discussed below.

[1] Information on material properties and choices listed here are credited to Prof. Verweij's group at the Ohio State Univ.

V. EXPLORATION OF STACKS FROM COMMERCIAL CERAMIC SHEETS

Recent investigations, carried out in close co-operation with Prof. Verweij have demonstrated that fully functional MPCs and DBEs may well be realized through advanced ceramic processing. It was found that use of anisotropic single crystals can be avoided by realizing artificial anisotropic dielectrics, exactly as in Fig. 11. The shown platelets consist of parallel arrangements of alternating ceramic beams. The ceramic route towards the manufacturing of A layers starts with stacking alternating layers of two different ceramics with low tanδ and largely different dielectric constants, ε. After an adhesion treatment, the stacks are sliced in perpendicular direction to form the "striped" composite A layer (Fig. 12).

The two ceramic compositions chosen for the laminate were α-Al_2O_3 with reported best values of $\varepsilon_r = 10$ and $\tan\delta = 2\times10^{-5}$ [19] and TiO_2 with reported best values of $\varepsilon_r = 100$ and $\tan\delta = 6\times10^{-5}$ [20]. Dense-ceramic Al_2O_3 sheets are commercially available. But since this is not the case for TiO_2, commercially available Ba-titanate (TD82) substrates were obtained that have a similar $\varepsilon_r \sim 82$ but a higher loss of $\tan\delta = 3.7\times10^{-4}$ at 2.13 GHz. The stacks are shown in Fig. 12. Without adhesive, they were found to have an anisotropic dielectric constant as predicted from mean field theory, and a loss $\tan\delta \sim 9.3\times10^{-4}$ at 8.36 GHz. This higher loss is likely related to the presence of absorbed water on the individual layers and effects of the interfacial gaps due to less than perfect flatness of the platelets.

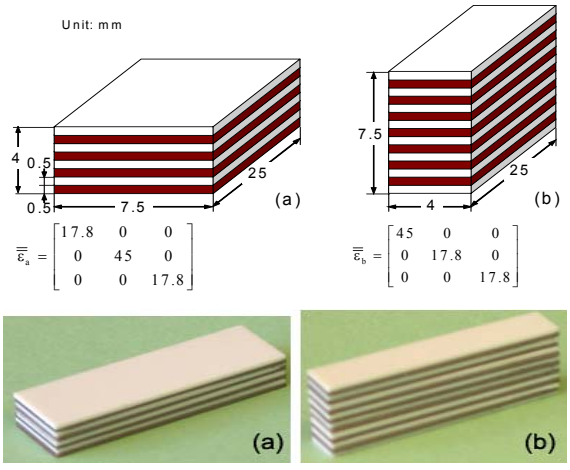

Fig. 11. *Upper*: geometry and theoretical dielectric tensor of two stacks, used for in-cavity dielectric measurements at the electro-science lab (ESL). The white and brown layers are Al_2O_3 and TD82 respectively. *Lower*: anisotropic dielectric laminates from commercial Al_2O_3|TD82 substrates, stacked without adhesive, and the same dimensions.

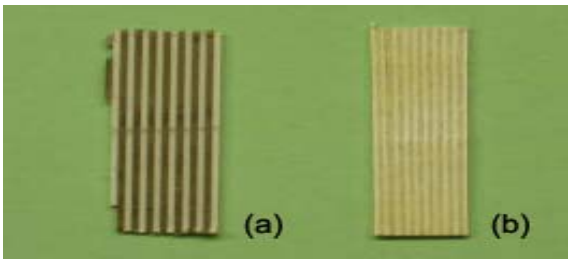

Fig. 12. 1 mm thick slices cut from (a) a commercial Al_2O_3|TD82 stack with organic adhesion and (b) a homemade Al_2O_3|TiO_2 stack with self-aligned, reactive adhesion.

The possibility to prepare striped layers was explored by Prof. Verweij's group using an organic polymer adhesive, followed by lamination. However, the organic adhesives were found to further increase the losses of the stacks to a $\tan\delta \sim 1.9\times10^{-3}$ for liquid adhesive (3M 4475) and 2.5×10^{-3} for double sided tape (3M 9492MP). The laminates were cut into 1 mm thick slices with a thin diamond blade using oil cooling. A first result is shown in Fig. 12a, but more focus is still necessary on avoiding deformation and in constructing materials that can exhibit loss tangents better than 10^{-5}.

VI. PRINTED CIRCUIT EMULATIONS OF ANISOTROPIC MATERIALS

Perhaps our most remarkable development in RF device miniaturization is the introduction of a novel pair of coupled printed microstrip lines (see Fig. 13) to emulate wave propagation within the usual DBE and MPC crystals. By adjusting the proximity of the microstrip lines or their width, emulation of the field growth and wave slow down can be done using standard of-the-shelf printed circuit technology. We have demonstrated this novel phenomenon using numerical tools and were able to show how small changes in parameters can be used to generate various k-w diagrams as shown in Fig. 14.

We can, thus, emulate propagation within crystals using a simple and easily realizable pair of transmission lines that may be allowed to couple with each other to generate the effects of the off-diagonal entries in the constituent permittivity tensors of the layered structure. This idea was demonstrated in [28] where we emulated a DBE dispersion diagram using the microstrip unit cell shown in Fig. 13. We demonstrated that by simply varying the width of one of the microstrip lines, various dispersion characteristics such as regular band edge (RBE) and double band edge (DbBE) crystals can be realized (See Fig. 14). The results in Fig. 14 were obtained using the analytical transfer matrices for coupled and uncoupled segments of the structure shown in Fig. 13

and enforcing the periodicity condition on the corresponding four ports of the structure.

The increase in field value within the coupled lines was demonstrated numerically as in Fig. 15 and can be exploited for high sensitivity antenna design. Two possible configurations are displayed in Fig. 16 and are the subject of future investigations.

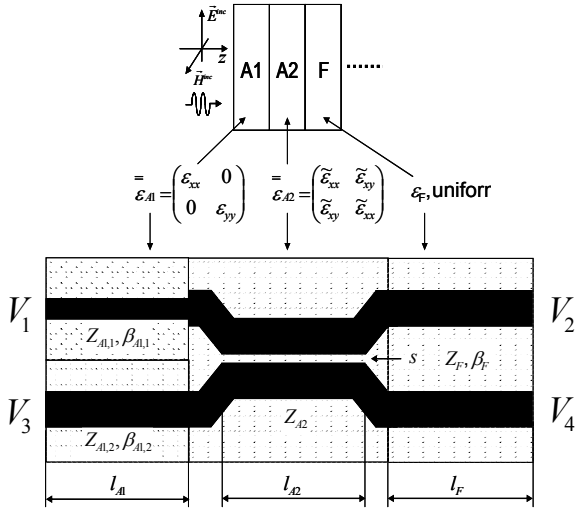

Fig. 13. A simple equivalent microstrip circuit for the three layers of the DBE and MPC crystals (patent pending).

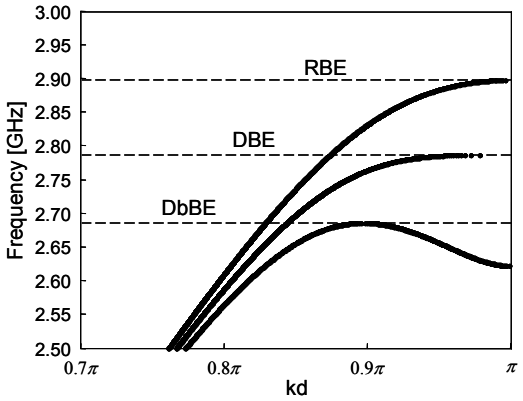

Fig. 14. Three distinct band edges can be realized by varying line #1 in Fig. 13.

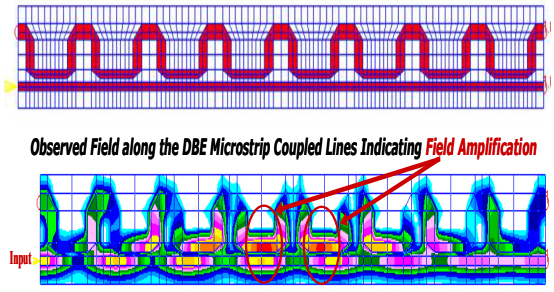

Fig. 15. Field distribution under the microstrip lines for an excitation at the DBE frequency.

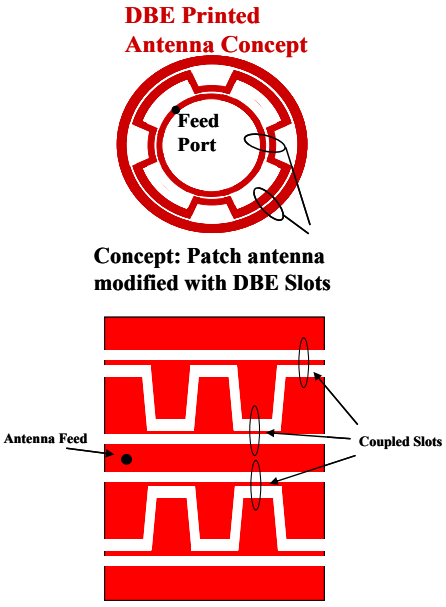

Fig. 16. DBE/MPC slot and patch antenna concepts.

VII. CONCLUSION

Material design capabilities offered by advances in dispersion engineering (including MPC/DBE crystals and negative index media) allow for unprecedented antenna and array designs possibilities. In this paper, we presented various avenues for antenna design using engineered materials. We specifically focused on MPCs and DBEs that support modes which can be harnessed to satisfy tight antenna design requirements. We summarized the properties of the frozen modes supported by these crystals and validated the existence of these modes with measurements. The paper concludes with the introduction of a simple coupled transmission line approach that emulates the dispersion and slow wave modes within the MPC and DBE crystals. Given the manufacturing simplicity of the printed coupled lines, the associated printed structures hold a great promise for realizing the advantages of the frozen modes.

ACKNOWLEDGEMENTS

This work was supported in part by the Air Force Office of Scientific Research under the MURI grant FA9550-04-1-0359 and the Office of Naval Research.

REFERENCES

[1] *IEEE Transactions on Antennas and Propagation*, Special Issue on Metamaterials, vol. 51, Oct. 2003.

[2] J. Joannopoulos, R. Meade, and J. Winn, "Photonic Crystals-Molding the Flow of Light," Princeton Univ. Press, 1995.

[3] S.-Y. Lin, E. Chow, V. Hietala, P. R. Villeneuve, and J. D. Joannopoulos, "Experimental demonstration of guiding and bending of electromagnetic waves in a photonic crystal," Science, vol. 282, pp. 274–276, Oct. 1998.

[4] H. Mosallaei and Y. Rahmat-Samii, "Periodic bandgap and effective dielectric materials in electromagnetics: Characterization and applications in nanocavities and waveguides*," IEEE Transactions on Antennas & Propagat.*, vol. 51, no. 3, pp. 549–563, Mar. 2003.

[5] E. Yablonovich, "Photonic band–gap crystals," *J. of Physics: Condensed Matter*, vol. 5, no. 16, pp. 2443–2460, Apr. 1993.

[6] D. R. Solli and J. M. Hickmann, "Photonic crystal based polarization control devices," *J. of Physics D: Applied Physics*, vol. 37, no. 24, pp. R263–R268, Dec. 2004.

[7] B. Temelkuran, M. Bayindir, E. Ozbay, R. Biswas, M. M. Sigalas, G. Tuttle, and K. M. Ho, "Photonic crystal based resonant antenna with a very high directivity," *J. of Applied Physics*, vol. 87, no. 1, pp. 603–605, Jan. 2000.

[8] R. Biswas, E. Ozbay, B. Temelkuran, M. Bayindir, M. M. Sigalas, and K. M. Ho, "Exceptionally directional sources with photonic–bandgap crystals," *J. of the Optical Society of America B*, vol. 18, no. 11, pp. 1684–1689, Nov. 2001.

[9] A. Erentok, P.L.Luljak, and R. W. Ziolkowski, "Characterization of a volumetric metamaterial realization of an artificial magnetic conductor for antenna applications," *IEEE Trans. Antennas & Propagat*., vol. 53, no. 1, pp. 160–172, Jan. 2005.

[10] M. Antoniades, F. Qureshi, and G. Eleftheriades, "Antenna Applications of Negative- Refractive-Index Transmission-Line Metamaterials," *2006 Int. Workshop on Antenna Technology, Conference Proceedings*, March 2006.

[11] A. Figotin and I. Vitebsky, "Nonreciprocal magnetic photonic crystals," *Physical Review E*, vol. 63, pp. 066–609,1–20, May 2001.

[12] A. Figotin and I. Vitebskiy, "Electromagnetic unidirectionality in magnetic photonic crystals," *Physical Review B*, vol. 67, pp. 165–210, 1–20, Apr. 2003.

[13] G. Mumcu, K. Sertel, J.L. Volakis, A. Figotin and I. Vitebsky, "RF propagation in finite thickness unidirectional magnetic photonic crystals," *IEEE T. Antenn. Propag.*, vol. 53, no. 12, pp. 4026-34, 2005.

[14] G. Mumcu, K. Sertel, and J.L. Volakis, "Miniature Antennas and Arrays Embedded within Magnetic Photonic Crystals" *IEEE Antennas and Wireless Propagat. Letters,* vol. 5, pp. 168 – 171, 2006.

[15] J. L. Volakis, C. C. Chen, M. Lee, and B. Kramer, "Miniaturization methods for narrowband and ultrawideband antennas," *IEEE international workshop on antenna Technology: Small Antennas and Novel Metamaterials, Marina Mandarin*, Singapore, Mar. 2005.

[16] A. Figotin and I. Vitebskiy, "Slow light in photonic crystals," arXiv:physics/0504112 vol. 2, Apr. 2005. (Topical Review, submitted to "Waves in Random and Complex Media").

[17] A. Figotin and I. Vitebsky, "Electromagnetic unidirectionality and frozen modes in magnetic photonic crystals," *J. Magnetism and Magnetic Materials* , vol. 300, no. 1, pp. 117-121, May 2006.

[18] S. Yarga, K. Sertel,and J. L. Volakis, "Degenerate Band Edge Crystals and Periodic Assemblies for High Gain Antennas," *submitted to IEEE Trans. Antennas & Propagat.* (see also paper by same authors in the 2006 IEEE Int. Symposium on Antennas and Propagat., Albuquereque, NM)

[19] N. M. Alford and S. J. Penn, "Sintered alumina with low dielectric loss," *J. Appl. Phys.*, vol. 80, no. 10, pp. 5895-98, 1996.

[20] A. Templeton, X. Wang, S. J. Penn, S. J. Webb, L. F. Cohen, and N. M. Alford, "Microwave dielectric loss of titanium oxide," *J. Am. Ceram. Soc.*, vol. 83, no. 1, pp. 95-100, 2000.

[21] M. Lee, C-C. Chen, and J. L. Volakis, "Distributed Lumped Loads and Lossy Transmission Line Model for Wideband Spiral Antenna Miniaturization and Characterization," *IEEE Trans. Antennas and Propagat.* (Submitted)

[22] B. A. Kramer, M. Lee, Chi-Chih Chen, and J. L. Volakis*, "*Design and Performance of an Ultra Wideband Ceramic-Loaded Slot Spiral," *IEEE Antennas and Propagat.* vol. 53, pp. 2193-2199, July 2005.

[23] M. Lee, B. A. Kramer, C-C. Chen, and J. L. Volakis, "Broadband Spiral Antenna Miniaturization Limit," *2006 IEEE Antennas and Propagation Society International Symposium*, Albuquerque, NM

[24] B. A. Kramer, C-C. Chen, and J. L. Volakis, "Miniature UWB Conformal Aperture via Volumetric Inductive Loading," *2006 IEEE Antennas and Propagation Society International Symposium*, Albuquerque, NM.

[25] L. J. Chu, "Physical limitations of antenna Q," *J. Appl. Phys.*, vol. 19, pp. 1163–1175, 1948.

[26] R. F. Harrington, "Effect of antenna size on gain, bandwidth, and efficiency," *J. Res. Nat. Bureau Stand.*, vol. 64D, pp. 1–12, Jan. 1960.

[27] B. Kramer, S. Koulouridis, C-C. Chen, and J. L. Volakis, "A Novel Reflective Surface for an UHF Spiral Antenna" *IEEE Trans. Antennas and Propagat. Letters,* vol. 5, pp. 32 – 34, 2006.

[28] C. Loecker, K. Sertel, and J. L. Volakis, "Emulation of Propagation in Layered Anisotropic Media with Equivalent Coupled Microstrip Lines," to appear in MWCL.

John L. Volakis was born on May 13, 1956 in Chios, Greece and immigrated to the U.S.A. in 1973. He obtained his B.E. Degree, summa cum laude, in 1978 from Youngstown State Univ., Youngstown, Ohio, the M.Sc. in 1979 from The Ohio State Univ., Columbus, Ohio and the Ph.D. degree in 1982, also from The Ohio State Univ.

From 1982-1984 he was with Rockwell International, Aircraft Division (now Boeing Phantom Works), Lakewood, CA and during 1978-1982 he was a Graduate Research Associate at the Ohio State University ElectroScience Laboratory. From January 2003 he is the Roy and Lois Chope Chair Professor of Engineering at the Ohio State University, Columbus, Ohio and also serves as the Director of the ElectroScience Laboratory (with ~$7M in research funding). Prior to moving to the Ohio State Univ, he was a Professor in the Electrical Engineering and Computer Science Dept. at the University of Michigan, Ann Arbor, MI. (1984-2003). He also served as the Director of the Radiation Laboratory from 1998 to 2000. His primary research deals with computational methods, electromagnetic compatibility and interference, design of new RF materials, multi-physics engineering and bioelectromagnetics. He has co-authored three books, 240 refereed journal papers, and over 340 conference papers. Dr. Volakis is listed by ISI among the top 250 most referenced authors (2004, 2005).

Dr. Volakis served as an Associate Editor of the *IEEE Transactions on Antennas and Propagation* from 1988-1992, and as an Associate Editor of Radio Science from 1994-97. He chaired the 1993 IEEE Antennas and Propagation Society Symposium and Radio Science Meeting, and co-chaired the same Symposium in 2003. Dr. Volakis was a member of the AdCom for the IEEE Antennas and Propagation Society from 1995 to 1998 and served as the 2004 President of the IEEE Antennas and Propagation Society. He also serves as an associate editor for the *J. Electromagnetic Waves and Applications,* the *IEEE Antennas and Propagation Society Magazine*, and the URSI Bulletin. He is a Fellow of the IEEE, and a member of Sigma Xi, Tau Beta Pi, Phi Kappa Phi, and Commission B of URSI. He is also listed in several Who's Who directories, including Who's Who in America.

Kubilay Sertel was born on June 27, 1973, in Tekirdag, Turkey. He received the B.S. degree from Middle East Technical University, Ankara, Turkey in 1995, the M.S. degree from Bilkent University, Ankara, Turkey in 1997, and the Ph.D. degree from the Electrical Engineering and Computer Science Department at the University of Michigan, Ann Arbor, MI in 2003, respectively.

He is currently a Senior Research Associate at the ElectroScience Laboratory at the Ohio State University. His research areas include electromagnetic theory, computational electromagnetics, volume-surface integral equations and hybrid methods, fast and efficient methods for large-scale electromagnetics problems and parallel implementations of fast algorithms.

Chi-Chih Chen received his BSEE in 1988 from National Taiwan University n Taiwan, MSEE and PhD degrees in 1993 and 1997, respectively, from The Ohio State University. He has been with The Ohio State University ElectroScience Laboratory (ESL) since 1993 as a Postdoctoral Researcher (1997~1999), Senior Research Associate (1999-2003) and Research Scientist in (2004~present). He is also an Adjunct Assistant Professor at The Ohio State University Electrical and Computer Engineering Department. Dr. Chen's research interests include ground penetrating radar technology, novel radar systems (vehicle obstacle detection, insect tracking, RFID, …), buried target detection/classification, UWB antenna designs, UWB dual-polarization feed/probe antenna designs for antenna and RCS ranges, miniature antenna designs for communication and navigation systems.